Life and Death of an Active Ethylene Polymerization Catalyst. Ligand Involvement in Catalyst Activation and Deactivation. Isolation and Characterization of Two Unprecedented Neutral and Anionic Vanadium(I) Alkyls

Damien Reardon,[†] Françoise Conan,[†] Sandro Gambarotta,*[,†] Glenn Yap,[†] and Qinyan Wang[‡]

Contribution from the Department of Chemistry, University of Ottawa, Ottawa, Ontario K1N 6N5, Canada, and NOVA Chemicals Corporation, 2928 16th Street N.E. Calgary, Alberta T2E 7K7, Canada

Received January 26, 1999

Abstract: Reaction of {2,6-bis[2,6-(i-Pr)$_2$PhN═C(Me)]$_2$(C$_5$H$_3$N)}VCl$_3$·1.3(CH$_2$Cl$_2$) (**1**) with stoichiometric amount of methyl alumoxane (PMAO) in toluene resulted in the methylation of the pyridine ring *ortho* position affording {2,6-bis[2,6-(i-Pr)$_2$PhN═C(Me)]$_2$(2-MeC$_5$H$_3$N)}VCl$_2$·0.5 (toluene) (**2**). In the process the ligand became an anionic amide, one chlorine atom was eliminated by the metal center, and the vanadium coordination number decreased by one unit. This new trivalent compound is a potent ethylene polymerization precatalyst, and polymers produced by the complex activated with PMAO showed a bimodal character in the GPC. Its bimodality is tentatively explained with the existence of two catalytically active species (mono and dialkylation of the vanadium center). Further attack of a strong alkylating agent such as MeLi occurs at the pyridine ring to either remove the methyl group, or to place an additional methyl group on the ring *meta* position. Both processes imply two-electron reduction of the metal center and formation of the corresponding V(I) derivatives {2,6-bis[2,6-(i-Pr)$_2$PhN═C (Me)]$_2$(C$_5$H$_3$N)}V(CH$_3$)(μ-CH$_3$)Li(Et$_2$O)$_3$ (**3**) and the ionic [{2,6-bis[2,6-(i-Pr)$_2$PhN═C(Me)]$_2$ (2,3-Me$_2$C$_5$H$_3$N)}V(CH$_3$)$_2$][Li(THF)$_2$(TMEDA)$_2$]·0.5(Et$_2$O) (**4**) which were isolated in crystalline form. Crystal data are as follows. **1**: monoclinic, space group *P2$_1$/n*, a = 18.267(5) Å, b = 16.643(4) Å, c = 38.195(9) Å, β = 96.061(5)°, Z = 12; **2**: monoclinic, space group *P2$_1$/c*, a = 15.741(2) Å, b = 16.565(2) Å, c = 15.849(2) Å, β = 100.316(3)°, Z = 4; **3**: orthorhombic space group *Pnma*, a = 19.724(6) Å, b = 22.001(7) Å, c = 11.035(3) Å, Z = 4; **4**: monoclinic space group *P2$_1$/n*, a = 11.932(3) Å, b = 25.363(6) Å, c = 18.957(4) Å, β = 96.587(4)°, Z = 4.

Introduction

Recent findings that a diimine/pyridine ligand system[1] spectacularly enhances the reactivity of electron-rich late-transition metals toward Ziegler−Natta olefin polymerization have attracted considerable attention in the literature. The very high activity of these catalysts and especially of those discovered by Brookhart[2] and Gibson[3] poses some fascinating questions about which particular ligand-to-metal bonding features may be responsible for the tremendous activity of these systems. Another point of interest arises from the nature of the polymer. Typically, these catalysts produce highly linear polymers with variable polydispersities.[4] Questions thus arise about which processes may determine chain initiation, termination, and molecular weight distribution in these highly active systems.

Our recent work on divalent samarium supported by tetradentate Schiff base ligands has indicated that it is possible for a coordinated diimine to be alkylated by nucleophilic agents.[5] As a result, the ligand became an anionic organic amide and the nature of the ligand/metal interaction was completely modified. In view of these findings, and since amide ligands have been proven to support Ziegler−Natta catalysts of early transition metals[6] and especially of vanadium,[7] we became thus interested in studying the catalytic activity of medium-valent vanadium complexes of neutral Schiff bases. For this work we

[†] University of Ottawa.

[‡] NOVA Chemicals Corporation.

(1) See, for example: (a) Johnson, L. K.; Mecking, S.; Brookhart, M. S. *J. Am. Chem. Soc.* **1996**, *118*, 267. (b) Johnson, L. K.; Killian, C. M.; Tempel, D. J.; Brookhart, M. S. *J. Am., Chem. Soc.* **1996**, *118*, 11664. (c) Johnson, L. K.; Killian, C. M.; Brookhart, M. S. *Organometallics* **1997**, *16*, 2005. (d) Guerin, F.; McConville, D. H.; Vittal, J. J.; Yap, G. P. A. *Organometallics* **1998**, *17*, 5172. (e) Etkin, N.; Ong, C. M.; Stephan, D. W. *Organometallics* **1998**, *17*, 3656.

(2) Johnson, L. K.; Killian, C. M.; Brookhart, M. S. *J. Am. Chem. Soc.* **1995**, *117*, 6414.

(3) Gibson, V. C.; Kimberley, B. S.; White, A. P. J.; Williams, D. J.; Howard, P. *J. Chem. Soc., Chem. Commun.* **1998**, 313.

(4) (a) Small, B. L.; Brookhart, M. S.; Bennett, A. M. A, *J. Am. Chem. Soc.* **1998**, *120*, 4049. (b) Britovsek, G. J. P.; Gibson, V. C.; Kimberley, B. S.; Maddox, P. J.; McTavish, S. J.; Solan, G. A.; White A. J. P.; Williams, D. J. *J. Chem. Soc., Chem. Commun.* **1998**, 849.

(5) Dubé, T.; Gambarotta, S.; Yap, G. P. A. *Organometallics* **1998**, *17*, 3967.

(6) (a) Boisson, C.; Berthet, J. C.; Ephritikhine, M.; Lance, M.; Nierlich, M. *J. Organomet. Chem.* **1997**, *531*, 115. (b) Witte, P. T.; Meetsma, A.; Hessen, B.; Budzelaar, P. T. H. *J. Am. Chem. Soc.* **1997**, *119*, 10561. (c) Kim, I.; Nishihara, Y.; Jordan, R. F.; Rogers, R. D.; Rheingold, A.; Yap, G. P. A. *Organometallics* **1997**, *16*, 3314. (d) Male, N. A. H.; Thornton-Pett, M.; Bochmann, M. *J. Chem. Soc., Dalton Trans.* **1997**, 2487. (e) Kim, I.; Jordan, R. F. *Macromolecules* **1996**, *29*, 489. (f) Scollard, J. D.; McConville, D. H. *J. Am. Chem. Soc.* **1996**, *118*, 10008.

(7) (a) Kim, W. K.; Fevola, M. J.; Liable-Sands, L. M.; Rheingold, A. L.; Theopold, K. H. I. *Organometallics* **1998**, *17*, 4541. (b) Brussee, E. A. C.; Meetsma, A.; Hessen, B.; Teuben, J. H. *Organometallics* **1998**, *17*, 4090. (c) Desmangles, N.; Gambarotta, S.; Bensimon, C.; Davis, S.; Zahalka, H. *J. Organomet. Chem.* **1997**, *562*, 53. (d) Murphy, V. J.; Turner, H. *Organometallics* **1997**, *16*, 2495.

10.1021/ja990263x CCC: $18.00
Published on Web 09/23/1999

have selected the same 2,6-bis[1-(2,6-dimethylphenylimino) ethyl]pyridine ligand[2,3] successfully used by Brookhart and Gibson for late transition metals. Our aim was 2-fold. First we wanted to probe the robustness of the particular diimine/pyridine ligand system mentioned above and its possible involvement in some of the transformations occurring during the catalytic cycle. Second, we wished to expand our understanding of the ability of d^2 vanadium complexes to function as olefin polymerization catalysts. It should be reiterated that, although a trivalent vanadium complex is one of the catalysts commercially used for the production of EPDM elastomers,[8] information remains surprisingly limited.[9]

Recently, we found that V(III) aryloxides work as potent Ziegler−Natta catalysts.[10] In close analogy to the catalytic system based on tris-diketonate vanadium, which is employed for the manufacture of EPDM rubber, the vanadium center undergoes reduction to the divalent state during the catalytic cycle. Formation of divalent vanadium typically results in catalyst failure and deactivation, and is a direct consequence of ligand abstraction by the Al cocatalyst.[11] In contrast, vanadium amide catalysts are more robust and are not so susceptible to reduction.[7c] One of the goals of this study was to verify the possibility that a ligand system containing a pyridine ring and two imino functions remains strongly bonded to the metal center during the cycle. By preventing ligand abstraction and consequent metal reduction, a considerable increase of the catalytic activity of the vanadium center could be reasonably anticipated.

In this paper, we describe the preparation and characterization of a trivalent vanadium diimine/pyridine complex as well as a preliminary assessment of its activity as a Ziegler−Natta precatalyst and an evaluation of the possible role played by the ligand in chain termination and catalyst deactivation.

Experimental Section

All operations were performed under inert atmosphere by using standard Schlenk type techniques. $VCl_3(THF)_3$[12] and 2,6-bis[1-(2,6-dimethylphenylimino)ethyl]pyridine[2] were prepared according to published procedures. Polyalumoxane solution (13.5% Al) in toluene (PMAO-IP, AKZO) was used as received. Infrared spectra were recorded on a Mattson 9000 and Nicolet 750-Magna FTIR instruments from Nujol mulls prepared in a drybox. Samples for magnetic susceptibility measurements were weighed inside a drybox equipped with an analytical balance and sealed into calibrated tubes. Magnetic measurements were carried out with a Gouy balance (Johnson Matthey) at room temperature. Magnetic moments were calculated following standard methods,[13] and corrections for underlying diamagnetism were applied to data.[14] Elemental analyses were carried out with a Perkin-Elmer 2400 CHN analyzer. Data for X-ray crystal structure determination were obtained with a Bruker diffractometer equipped with a SMART CCD area detector.

Preparation of {2,6-bis[2,6-(i-Pr)$_2$PhN=C(Me)]$_2$(C$_5$H$_3$N)}VCl$_3$·1.3(CH$_2$Cl$_2$) (1). A solution of $VCl_3(THF)_3$ (1.6 g, 4.1 mmol) in anhydrous THF (100 mL) was treated with 2,6-bis[1-(2,6-diisopropylphenylimino)ethyl]pyridine (2.0 g, 4.1 mmol). The solution was heated to 70 °C for 1 h and then stirred overnight at room temperature. The color of the solution changed from cherry-red to burgundy. The solvent was evaporated under reduced pressure to yield a dark red solid which was redissolved in anhydrous CH_2Cl_2 (75 mL). Dark red crystals of **1** were obtained after allowing the resulting solution to stand 3 days at room temperature (2.77 g, 3.7 mmol, yield 90%). IR (Nujol mull, cm^{-1}): 3163 (m), 3059 (s), 2012 (w), 1936 (w), 1876 (w), 1574 (s), 1328 (m), 1317 (m), 1267 (s), 1206 (s), 1179 (m), 1149 (w), 1105 (m), 1057 (m), 1038 (m), 980 (w), 954 (w), 937 (m), 905 (w), 834 (w), 815 (m), 797 (s), 777 (s), 758 (w), 746 (m), 723 (w), 697 (w), 651 (w), 618 (w), 560 (w). Anal. Calcd (found) for $C_{34.33}H_{45.67}Cl_{5.67}N_3V$: C 54.81 (54.73), H 6.12 (6.01), N 5.59 (5.47). $\mu_{eff} = 2.94\ \mu_B$.

Preparation of {2,6-bis[2,6-(i-Pr)$_2$PhN=C(Me)]$_2$(2-MeC$_5$H$_3$N)}-VCl$_2$·0.5 hexane (2). A suspension of **1** (2.1 g, 3.3 mmol) in anhydrous toluene (150 mL) was treated with PMAO (0.8 mL, 13% Al solution in toluene, 6.6 mmol). The color rapidly changed from red to green. The mixture was gently heated and allowed to stir for 16 h at room temperature. The resulting suspension was filtered to eliminate a small amount of insoluble material. After the solvent was evaporated in vacuo, the green, solid residue was dissolved in anhydrous CH_2Cl_2 (40 mL) and layered with hexane (40 mL). Dark green crystals of **2** (0.63 g, 0.95 mmol, yield 29%) separated upon standing undisturbed at room temperature for 14 days. IR (Nujol mull, cm^{-1}): 3187 (s), 1612 (m), 1588(w), 1565 (m), 1517 (m), 1414 (w), 1364 (m), 1351 (m), 1324 (w), 1308 (w), 1260 (s), 1187 (m), 1146 (m), 1099 (s), 1054 (s), 1022 (s), 934 (w), 909 (w), 863 (m), 804 (s), 772 (s), 754 (w), 720 (m), 695 (m), 672 (m), 650 (w), 570 (w). Anal. Calcd (found) for $C_{37}H_{53}N_3VCl_2$: C 67.16 (66.93), H 8.07 (7.84), N 6.35(6.21). $\mu_{eff} = 2.87\ \mu_B$.

Method B. A solution of **1** (1.31 g, 2.0 mmol) in anhydrous toluene (100 mL) was cooled to −78 °C. The addition of a solution of MeLi in ether (1.43 mL, 1.4 M, 2.0 mmol) to the mixture immediately changed the color from red to green. The solution was allowed to warm slowly to room temperature and then stirred for 4 h at room temperature. The solvent was removed in vacuo to yield a dark green, solid residue which was redissolved in ether (100 mL). The resulting solution was filtered to remove a small quantity of insoluble material, and a small amount of hexane was added. Dark green crystals of **2** separated upon standing at −30 °C for 72 h (0.68 g, 1.1 mmol, 54%).

Preparation of {2,6-bis[2,6-(i-Pr)$_2$PhN=C(Me)]$_2$(C$_5$H$_3$N)}V(CH$_3$)-(μ-CH$_3$)Li(Et$_2$O)$_3$ (3). A solution of **1** (1.3 g, 2.0 mmol) in anhydrous toluene (100 mL) was cooled to −78 °C. The addition of a solution of MeLi in ether (5.7 mL, 1.4 M, 8.0 mmol) immediately changed the color of the mixture from red to dark brown. The solution was allowed to warm slowly to room temperature and then stirred for additional 4 h. The solvent was then removed in vacuo to yield a dark brown solid which was redissolved in freshly distilled ether (100 mL). The solution was filtered to remove a small quantity of insoluble material. Dark brown crystals of **3** separated upon allowing the solution to stand at room temperature for 72 h (0.83 g, 1.0 mmol, yield 50%). IR (Nujol mull, cm^{-1}): 3167 (m), 3050 (m), 1611 (m), 1585(w), 1457(s), 1378 (m), 1312 (m), 1246 (s), 1199 (m), 1189 (m), 1174 (w), 1153 (w), 1102 (w), 1092 (m), 1055 (s), 1042 (s), 986 (w), 952 (m), 934 (w), 889 (w), 861 (w), 825 (w), 803 (m), 775 (m), 758 (m), 738 (m), 722 (m), 694 (w), 682 (w), 629 (w). Anal. Calcd (found) for $C_{47}H_{79}O_3N_3VLi$: C 71.27 (71.02), H 10.05 (9.89), N 5.31 (5.26). $\mu_{eff} = 2.50\ \mu_B$.

Preparation of [{2,6-bis[2,6-(i-Pr)$_2$PhN=C(Me)]$_2$(2,3-Me$_2$C$_5$H$_3$N)}-V(CH$_3$)$_2$][Li(THF)$_2$ (TMEDA)$_2$]·0.5(Et$_2$O) (4). A solution of **1** (1.3 g, 2.0 mmol) in anhydrous toluene (100 mL) was cooled to −78 °C. The addition of a solution of MeLi in ether (5.7 mL, 1.4 M, 8.0 mmol) changed immediately the color of the mixture from red to dark brown.

(8) (a) Doi, Y.; Suzuki, S.; Soga, K. *Macromolecules* **1986**, *19*, 2896. (b) Ouzumi, T.; Soga, K. *Makromol. Chem.* **1992**, *193*, 823. (c) Gumboldt, A.; Helberg, J.; Schleitzer, G. *Makromol. Chem.* **1967**, *101*, 229. (d) Adisson, E. *J. Polym. Sci., Part A: Polym. Chem.* **1994**, *32*, 1033. (e) Davis, S. C.; von Hellens, W.; Zahalka, H. In *Polymer Material Encyclopedia;* Salamone, J. C., Ed.; CRC Press Inc., 1996; Vol. 3.

(9) (a) Schuere, S.; Fisher, J.; Kress, J. *Organometallics* **1995**, *14*, 2627. (b) Zambelli, A.; Proto, A.; Longo, P. In *Ziegler Natta Catalysis*; Fink, G., Mulhaupt, R., Brintzinger, H. H., Eds.; Springer-Verlag: Berlin, 1995. (c) Kim, W. K.; Fevola, M. J.; Liable-Sands, L. M.; Rheingold, A. L.; Theopold, K. H. *Organometallics* **1998**, *17*, 4541. (d) Feher, K. J.; Walzer, J. F.; Blanski, R. L. *J. Am. Chem. Soc.* **1991**, *113*, 3618. (e) Czaja, K.; Bialek, M. *Macromol. Rapid Commun.* **1998**, *19(3)*, 163−166. (f) Buhl, M. *Angew. Chem. Int. Ed.* **1998**, *37(1−2)*, 142−144. (g) Chan, M. C. W.; Cole, J. M.; Gibson, V. C.; Howard, J. A. K. *J. Chem. Soc. Chem. Commun.* **1997**, 2345.

(10) Kasani, A.; Ruppa, K. B.; Gambarotta, S.; Yap, G. P. A., manuscript in preparation.

(11) Ma, Y.; Reardon, D.; Gambarotta, S.; Yap, G. P. A.; Zahalka, H.; Lemay, C. *Organometallics*, manuscript submitted for publication.

(12) Manzer, L. E. *Inorg. Synth.* **1982**, *21*, 138.

(13) Mabbs, M. B.; Machin, D. *Magnetism and Transition Metal Complexes*; Chapman and Hall; London, 1973.

(14) Foese, G.; Gorter, C. J.; Smits, L. J. *Constantes Selectionnées Diamagnetisme, Paramagnetisme, Relaxation Paramagnetique;* Masson: Paris, 1957.

Table 1. Polymerization Results

entry	*T* (°C)	activation	run time (min)	yield (g)	activity (1) g PE/mmol cat·hr	activity (2) g PE/mmol cat·[C2]·hr	MW ($\times 10^{-3}$)	PD
1	50	PMAO (Al/V = 600)	15	22.8	1415.6	652.4	67.4	11.54
2[a]	50	PMAO (Al/V = 60)	30	24.2	2243.5	3309.9	174.2	50.79
3	140	PMAO (Al/V = 600)	10	6.6	611.7	788.8	277.6	40.35
4	140	PMAO (Al/V = 60)	10	6.3	583.9	752.9	178.9	35.92
5[b]	140	PMAO (Al/V = 60)	10	5.6	519.0	669.2	179.2	30.90
6[c]	140	PMAO (Al/V = 20) $B(C_6F_5)_3$ (B/V = 1.05)	10	3.3	305.0	393.3	58.3	8.46

[a] In this particular case the catalyst concentration was 100 μmol/L instead of 300 μmol/L in all other cases. The ethylene total pressure was 100 psig. The temperature was controlled within 5 °C. [b] 40 mL of 1-octene was added into reactor in a batch. 3.9 Br/1000C was detected by FT-IR; polymer melting point was 127.4 °C. [c] PMAO and the catalyst (Al/V = 20) were premixed before injected into the reactor. The catalyst and $B(C_6F_5)_3$ solution were injected into the reactor simultaneously.

The solution was allowed to warm slowly to room temperature and then stirred for additional 72 h. The solvent was then removed in vacuo to yield a dark brown solid which was redissolved in freshly distilled ether (100 mL) followed by the addition of TMEDA (2 mL) and THF (10 mL). The resulting solution was filtered to remove a small amount of insoluble material. Dark brown crystals of **4** were obtained upon allowing the resulting solution to stand at room temperature for 72 h. (0.78 g, 0.86 mmol, yield 44%). IR (Nujol mull, cm^{-1}): 3168(m), 3050-(m), 2924(s), 2853(s), 1585(m), 1457(s), 1378(s), 1312(m), 1245(s), 1200(w), 1190(w), 1174(w), 1154(w), 1102(m), 1099(s), 1092(m), 1055(m), 1042(w), 986(w), 953(m), 934(m), 890(w), 861(w), 825(m), 803(m), 775(m), 758(m), 738(w), 722(m), 695(w), 682(w), 629(w). Anal. Calcd (found) for $C_{53}H_{92}N_5O_{2.5}VLi$: C 70.95(70.88), H 10.34 (10.11), N 7.81(7.65). $\mu_{eff} = 2.64\ \mu_B$.

General Polymerization Procedure. Ethylene (99.5%, polymer grade, Praxair) was purified by passage through the bench scale reactor's gas purification units (13× molecular sieves, alumina and oxygen removal columns). Anhydrous toluene was purchased from Aldrich and purified over molecular sieves prior to use. PMAO-IP was purchased from Akzo-Nobel and contained 13.5 wt % of Al. $B(C_6F_5)_3$ was purchased from Boulder Scientific Inc. and used without further purification.

A bench scale reactor was used in the polymerization experiments. The reactor uses a programmable logic control (PLC) system with Wonderware 5.1 software for process control. Ethylene polymerizations were performed in the 500 mL Autoclave Engineers Zipperclave reactor equipped with an air driven stirrer and an automatic temperature control system. All of the chemicals were fed into the reaction batchwise except for ethylene which was fed on demand.

Conditions for polymerization.

	slurry phase	solution phase
toluene	216 mL	216 mL
catalyst concentration	300 μmol/L	300 μmol/L
PMAO	Al/V = 600 (mol/mol)	Al/V = 60, 600 (mol/mol)
reaction temperature	50 °C	140 °C
reactor pressure	300 psig total	286 psig total

As summarized above, the control temperature was 50 °C for a slurry polymerization and 140 °C for solution polymerization experiments. The polymerization time varied from 10 to 30 min. The reaction was terminated by adding 5 mL of methanol to the reactor, and the polymer was recovered by evaporation of the toluene in vacuo. The polymerization activities were calculated based upon weight of polymer produced (Table 1).

Polymer molecular weights and molecular weight distributions were measured by GPC (Waters 150-C) at 140 °C in 1,2,4-trichlorobenzene calibrated using polyethylene standards. DSC was conducted on a DSC 220 C from Seiko Instruments. The heating rate was 10 °C/min from 0 to 200 °C.

In a typical polymerization experiment, the solvent was presaturated with ethylene in the reactor at the desired temperature. The cocatalyst was injected in the reactor followed by introduction of the precatalyst. In the mixed-activator experiment the two cocatalysts were premixed and injected in the reactor prior to introduction of the precatalyst. 1-octene was introduced in the reactor and premixed with ethylene before heating. Reproducibility of catalyst activity and reactor operation was checked by regularly running polymerization experiments using a standard zirconium catalyst and by repeating the experiments under identical reaction conditions. Errors and deviation were always below 5.9%.

X-ray Crystallography. Suitable crystals were selected, mounted on thin glass fibers using paraffin oil and cooled to the data collection temperature. Data were collected on a Bruker AX SMART 1k CCD diffractometer using 0.3° ω-scans at 0, 90, and 180° in ϕ. Unit-cell parameters were determined from 60 data frames collected at different sections of the Ewald sphere. Semiempirical absorption corrections based on equivalent reflections were applied.

Systematic absences in the diffraction data and unit-cell parameters were consistent, uniquely, with the reported space group for **1**, **2**, and **4** and with $Pna2_1$ ($Pn2_1a$), and *Pnma* for **3**. Solution in *Pnma* yielded chemically reasonable and computationally stable results of refinement for **3**. The structures were solved by direct methods, completed with difference Fourier syntheses and refined with full-matrix least-squares procedures based on F^2. Three symmetry-unique but chemically equivalent molecules of the complex and four molecules of methylene chloride solvent, one of which is disordered with a 60/40 site occupation distribution were located in the asymmetric unit of **1**. A molecule of hexane solvent was located in **2** disordered at an inversion center and was refined with half site occupancy. A half molecule of diethyl ether solvent and a lithium counterion, coordinated with one TMEDA and two THF ligand molecules, were located in **4**. A lithium ion, coordinated to three diethyl ether molecules, was located within interacting distance of one of the methyl ligands of the anionic complex in **3**. All non-hydrogen atoms were refined with anisotropic displacement parameters. All hydrogen atoms were treated as idealized contributions. All scattering factors and anomalous dispersion factors are contained in the SHEXTL 5.03 program library. Crystal data and relevant geometrical parameters are reported in Tables 2 and 3, respectively.

Complex 1. The structure of **1** consists of a vanadium atom surrounded by the pyridine/diimine ligand and three chlorine atoms (Figure 1). The coordination geometry around the metal center is distorted octahedral with the equatorial plane defined by the three nitrogen atoms of the ligand [N(1)−V(1)−N(2) = 74.61(13)°, N(2)−V(1)−N(3) = 75.46(13)°, N(1)−V(1)−N(3) = 150.03(12)°] and one chlorine atom [N(1)−V(1)−Cl(1)= 106.07(10)°, N(3)−V(1)−Cl(1) = 103.90(10)°, N(2)−V(1)−Cl(1) = 177.43(11)°]. The other two chlorine atoms are placed on the two axial positions and form a significantly bent Cl−V−Cl vector [Cl(2)−V(1)−Cl(3) = 166.38(6)°]. The V−Cl

Table 2. Crystal Data and Structure Analysis Results

	1	2	3	4
formula	$C_{33}H_{43}Cl_3N_3V$ 1.3(CH_2Cl_2)	$C_{34}H_{46}Cl_2N_3V$ 0.5(hexane)	$C_{47}H_{79}LiN_3O_3V$	$C_{51}H_{87}LiN_5O_2V$ 0.5(ether)
formula weight	752.23	661.66	792.01	897.20
crystal system	monoclinic	monoclinic	orthorhombic	monoclinic
space group	$P2_1/n$	$P2_1/c$	*Pnma*	$P2_1/n$
a (Å)	18.267(5)	15.741(2)	19.724(6)	11.932(3)
b (Å)	16.643(4)	16.565(2)	22.001(7)	25.362(6)
c (Å)	38.195(9)	15.849(2)	11.035(3)	18.957(4)
β (deg)	96.061(5)	100.316(3)		96.587(4)
V (Å^3)	11547(5)	4066.0(9)	4789(3)	5699(2)
Z	12	4	4	4
radiation (Kα)	0.71073 Å	0.71073 Å	0.71073 Å	0.71073 Å
T (K)	226	203	204	213
D_{calcd} (g cm^{-3})	1.298	1.081	1.099	1.046
μ_{calcd} (mm^{-1})	0.678	0.401	0.246	0.214
F_{000}	4704	1412	1728	1964
R, R_w[2] [a]	0.0548, 0.1573	0.074, 0.1954	0.0863, 0.2279	0.1148, 0.2280
G.O.F	1.110	1.069	1.002	1.019

[a] $R = \sum(F_o - F_c)/\sum F_o$. $R_w = [(\sum(F_o - F_c)^2/\sum wF_o2)]^{1/2}$.

Table 3. Selected Bond Distances (Å) and Angles (deg)

1	2	3	4
V(1)−Cl(1) = 2.2739(14)	V−Cl(1) = 2.257(2)	V−C(1) = 2.118(7)	V−C(1) = 2.075(11)
V(1)−Cl(2) = 2.2924(14)	V−Cl(2) = 2.259(2)	V−C(2) = 2.093(9)	V−C(2) = 2.115(10)
V(1)−Cl(3) = 2.3552(14)	V−N(1) = 2.162(6)	V−N(1) = 1.911(6)	V−N(1) = 1.986(9)
V(1)−N(1) = 2.242(3)	V−N(2) = 1.886(6)	V−N(2) = 2.046(4)	V−N(2) = 1.872(9)
V(1)−N(2) = 2.067(3)	V−N(3) = 2.156(6)	Li−C(1) = 2.514(18)	V−N(3) = 2.005(9)
V(1)−N(3) = 2.212(3)	C(19)−C(34) = 1.561(9)		C(17)−C(18) = 1.602(15)
N(1)−C(13) = 1.283(15)			C(19)−C(20) = 1.552(14)
N(3)−C(20) = 1.288(5)			
N(1)−V(1)−Cl(1) = 106.07(10)	N(1)−V−N(3) = 154.2(3)	V−C(1)−Li = 151.4(5)	C(1)−V−C(2) = 111.4(5)
N(1)−V(1)−Cl(2) = 88.96(9)	N(1)−V−N(2) = 78.6(3)	C(1)−V−C(2) = 119.9(3)	C(1)−V−N(3) = 95.9(4)
N(1)−V(1)−Cl(3) = 89.25(9)	N(1)−V−Cl(1) = 98.74(18)	C(1)−V−N(1) = 96.6(3)	C(1)−V−N(2) = 102.3(4)
N(1)−V(1)−N(2) = 74.61(13)	N(1)−V−Cl(2) = 96.30(17)	C(1)−V−N(2) = 98.55(13)	C(1)−V−N(1) = 108.2(4)
N(2)−V(1)−Cl(1) = 177.43(11)	Cl(1)−V−Cl(2) = 112.10(9)	C(2)−V−N(2) = 95.71(15)	C(2)−V−N(1) = 93.8(4)
Cl(2)−V(1)−Cl(3) = 166.38(6)	Cl(1)−V−N(2) = 113.69(18)	C(2)−V−N(1) = 143.5(3)	C(2)−V−N(2) = 146.0(4)
N(3)−C(20)−C(19) = 116.9(4)	Cl(2)−V−N(2) = 134.18(19)	N(2)−V−N(1) = 77.53(13)	C(2)−V−N(3) = 92.9(4)
N(1)−V(1)−N(3) = 150.03(12)	N(2)−C(19)−C(34) = 109.1(6)	N(2)−V−N(2a) = 151.1(2)	N(1)−V−N(3) = 150.5(4)
N(2)−V(1)−N(3) = 75.46(13)	C(20)−C(19)−C(18) = 114.6(7)		N(2)−C(17−-C(18) = 106.4(10)
	N(3)−C(20)−C(19) = 115.5(7)		N(2)−C(17)−C(15) = 104.4(11)

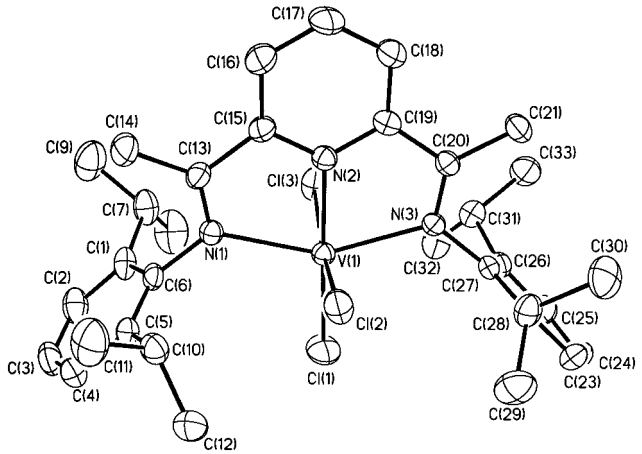

Figure 1. Thermal ellipsoid plot of 1. Thermal ellipsoids are drawn at the 30% probability level.

distances [V(1)−Cl(1) = 2.2739(14) Å, V(1)−Cl(2) = 2.2924(14) Å, V(1)−Cl(3) = 2.3552(14) Å] are slightly different from each other but fall in the expected range for terminal V−Cl bonds. The V−N distances are also normal. The two V−N distances formed by the two imine functions [V(1)−N(1) = 2.242(3) Å, V(1)−N(3) = 2.212(3) Å] are longer than that formed with the pyridine nitrogen atom [V(1)−N(2) = 2.067(3) Å] possibly suggesting the presence of some extent of V−pyridine π-bonding. The C−N bonds of the two imine groups are only slightly longer than expected [N(1)−C(13) = 1.283(5) Å, N(3)−C(20) = 1.288(5) Å]. The pyridine ring is coplanar with the molecular equatorial plane whereas the two terminal phenyl groups attached to the two imino nitrogens lay on perpendicular planes.

Complex 2. The coordination geometry of vanadium in this complex can be described as distorted trigonal bipyramidal and is defined by two chlorine atoms and by the three nitrogen donor atoms of the tridentate ligand (Figure 2). Two chlorines and the nitrogen atom of the methylated pyridine ring define with the metal center the molecular equatorial plane [Cl(1)−V−Cl(2) = 112.10(9)°, Cl(1)−V−N(2) = 113.69(18)°, Cl(2)−V−N(2) = 134.18(19)°]. Two nitrogens of the two imino functions are located on the axial position forming a significantly bent N−V−N vector [N(1)−V−N(3) = 154.2(3)°]. Apart from the deviation from the planarity of the methylated pyridine ring, the diimine/pyridine ligand does not display additional distortion with respect to complex **1**. Even the V−Cl [V−Cl(1) = 2.257(2) Å, V−Cl(2) = 2.259-(2) Å] as well as the V−N bond distances [V−N(1) = 2.162(6) Å, V−N(3) = 2.156(6) Å] compare well to those of complex **1**. Conversely, the V−N distance with the distorted ring [V−N(2) = 1.886(6) Å] is shorter as a result of the change of the nature of the V−N interaction and the presence of a formal negative charge on the ring. Similar to complex **1** the orientation of the two peripheral phenyl rings is perpendicular to the V−N(1)−N(2)−N(3) plane. The decrease of the vanadium coordination number with respect to **1** does not significantly affect the geometry of the vanadium/diimine core.

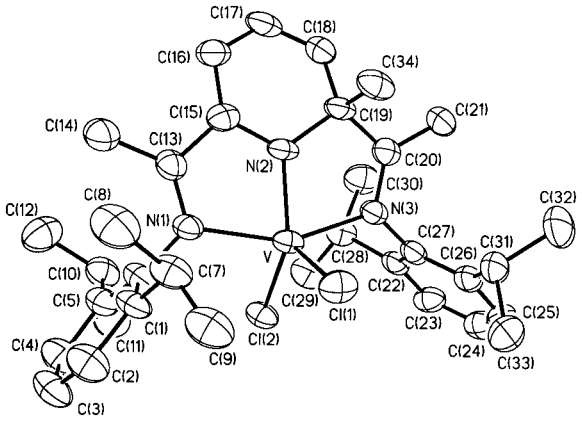

Figure 2. Thermal ellipsoid plot of **2**. Thermal ellipsoids are drawn at the 30% probability level.

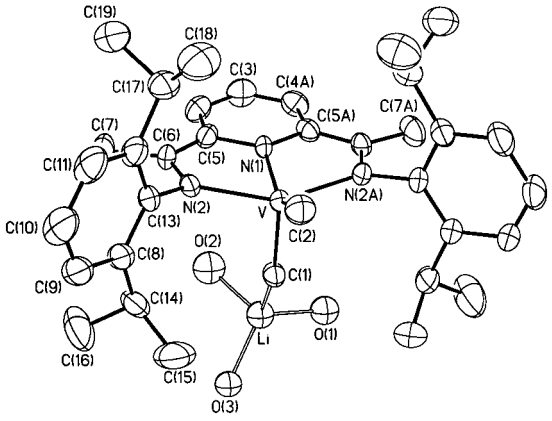

Figure 3. Thermal ellipsoid plot of **3**. Thermal ellipsoids are drawn at the 30% probability level.

Complex 3. The coordination geometry around the vanadium center is in this case better described as square pyramidal (Figure 3) and is strongly reminiscent of the recently reported structure of the $FeCl_2$ adduct of the same ligand.[4] The three nitrogen donor atoms of the ligand and one terminal methyl group define the basal plane [N(1)−V−N(2) = 77.53(13)°, N(1)−V−C(2) = 143.5(3)°, N(2)−V−C(2) = 95.71-(15)°, N(2)−V−N(2a) = 151.1(2)°]. The vanadium atom is slightly elevated above the plane [distance from the plane 0.51 Å] while a second methyl group occupies the axial position. The V−N distances [V−N(2) = 2.046(4) Å] are normal and compare well with those of complex **1**. The pyridine ring forms a V−N distance [V−N(1) = 1.911-(6) Å] which is longer than in complex **2** but which compares well to that of **1**. The V−C distances [V−C(1) = 2.118(7) Å, V−C(2) = 2.093-(9) Å] slightly differ from each other as a probable result of the different positions in the coordination polyhedron (basal versus axial). One tetrahedral lithium atom attached to three molecules of coordinated ether [Li−O(1) = 1.934(15) Å] is also bonded to the axial methyl group [Li−C(1) = 2.514(18) Å] forming a significantly bent Li−C−V vector [V−C(1)−Li = 151.4(5)°].

Complex 4. Despite the considerable distortion of the diimine ligand pyridine ring introduced by the double methylation, the coordination geometry around the vanadium center (Figure 4) is very similar to that observed in complex **3** [N(1)−V−N(2) = 79.7(4)°, N(1)−V−N(3) = 150.5(4)°, N(1)−V−C(2) = 93.8(4)°, N(2)−V−C(2) = 146.0(4)°, N(3)−V−N(2) = 78.7(4)°, N(3)−V−C(2) = 92.9(4)°]. Even in this case, the coordination geometry around the metal center is square pyramidal with the three nitrogen donor atoms [V−N(1) = 1.986(9) Å, V−N(2) = 1.872(9) Å, V−N(3) = 2.005(9) Å] and one methyl group [V−C(2) = 2.115(10) Å] defining the basal plane. The vanadium atom is elevated above the basal plane [distance from the plane 0.50 Å] and all of the bond distances and angles compare rather well to those of **3**. The second methyl is placed on the axial position [C(1)−V−C(2) = 111.4(5)°, C(1)−V−N(1) = 108.2(4)°, C(1)−V−N(2) = 102.3(4)°, C(1)−V−N(3) = 95.9(4)°] forming a V−C distance [V−C(1) = 2.075(11) Å] which compares well with that of complex **3**. This is in spite of the fact that the lithium countercation is solvated by one molecule of TMEDA [Li−N(4) = 2.11(3) Å] and two molecules of THF [Li−O(1) = 1.93(2) Å] and does not form a direct bonding interaction with the anionic vanadium moiety.

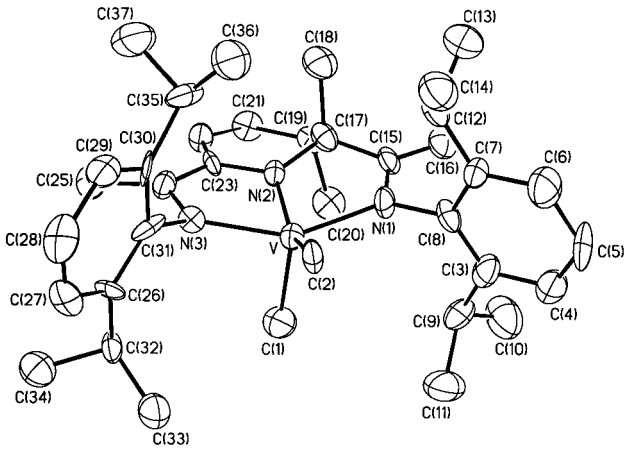

Figure 4. Thermal ellipsoid plot of **4**. Thermal ellipsoids are drawn at the 30% probability level.

Scheme 1

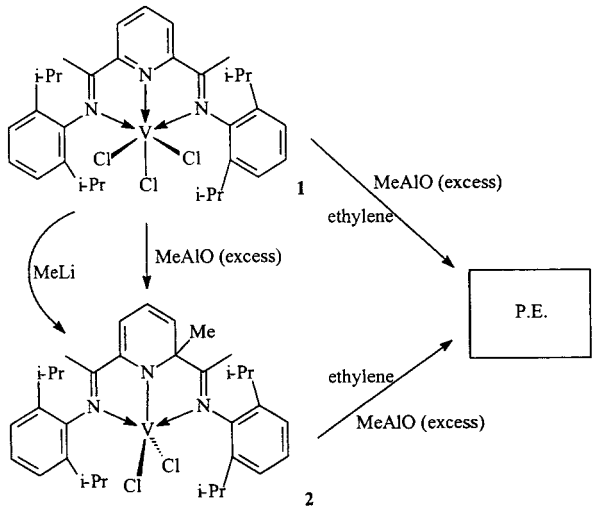

Results and Discussion

Reaction of $VCl_3(THF)_3$ with 2,6-bis[1-(2,6-dimethylphenylimino)ethyl]pyridine in toluene afforded a dark red, scarcely soluble solid of the trivalent and mononuclear adduct 2,6-[(2,6-$(i\text{-}Pr)_2C_6H_3N)C(CH_3)]_2C_5H_3NVCl_3$ (**1**) (Scheme 1). The complex is paramagnetic and shows a magnetic moment as expected for the d^2 electronic configuration of the trivalent vanadium center. Not surprising, complex **1** is a potent ethylene polymerization catalyst precursor (Table 1). However, when comparing the activity to literature data, it appears that when **1** is activated with methyl alumoxane (PMAO), the catalyst productivity is somewhat lower than that displayed by the related Fe derivative recently reported by Brookhart and Gibson.[4] Upon mixing a red toluene solution of **1** with excess of methyl alumoxane cocatalyst, the color immediately turned emerald green and vigorous ethylene uptake took place to form linear polyethylene as indicated by the melting point of the polymer (132.1 °C). When complex **1** was activated with PMAO at 50 °C and with a ratio Al/V = 600 (entry 1), the polymerization under slurry conditions started immediately, and the temperature of the

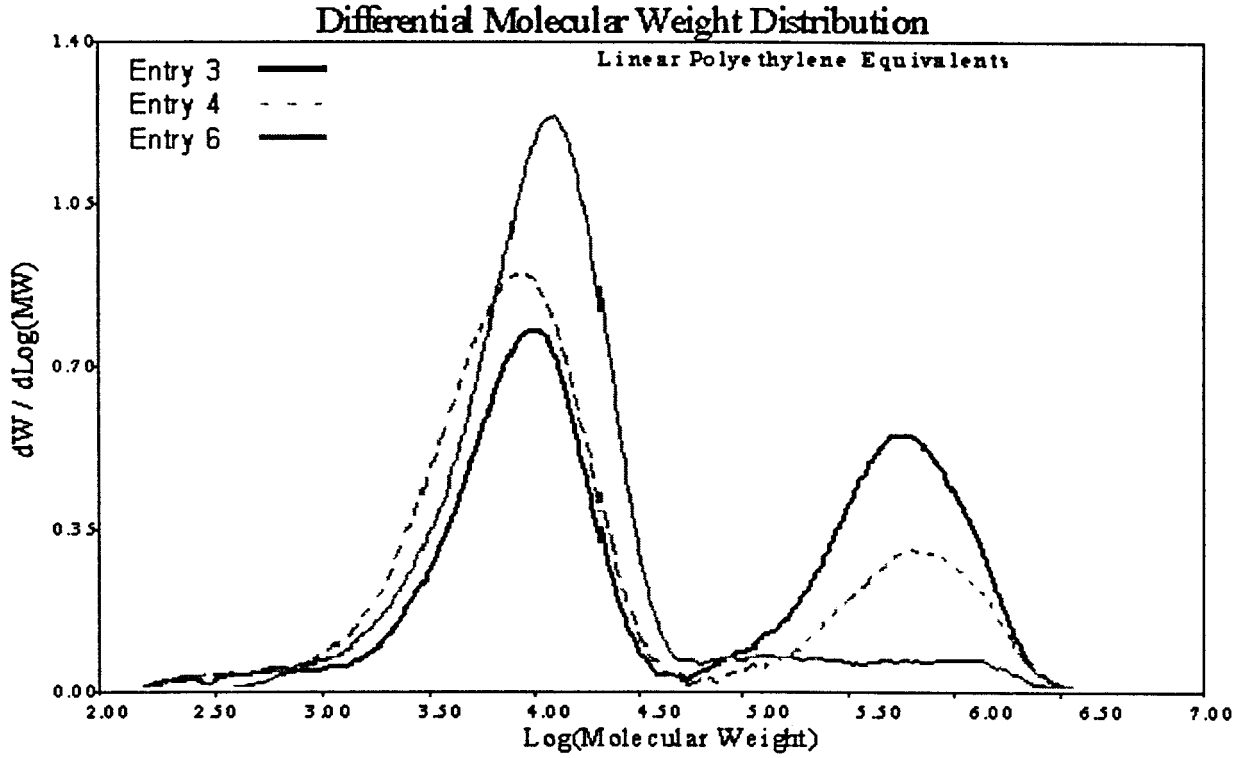

Figure 5. Gel permeation chromatogram of **1** at 140 °C (entry 3, 4, and 6).

reaction mixture increased from 50 to about 85 °C within 20 s. The initial polymerization rate was high, but ethylene consumption slowed after about 2 min. However, the catalyst remained active throughout the 15 min run. This phenomenon might be caused by embedding of catalyst sites in the solid polyethylene produced during the first few minutes. The GPC showed polymers with high polydispersities (Table 1). Deconvolution of the GPC curve revealed one main peak which can be attributed to a single catalyst species. A comparison of the runs conducted at different temperatures and under two different reaction conditions (slurry and solution phase) showed that the overall polymerization productivity is similar. However, the reactions carried out at two different temperatures displayed totally different kinetic profiles. The catalyst showed an extended life at 50 °C but was deactivated within 1 min at 140 °C. A bimodal character is clearly apparent in the GPC curves for polymers obtained at 140 °C using PMAO as cocatalyst (Figure 5). We observed that a higher Al/V ratio favored the formation of the catalytic species responsible for the formation of high-molecular-weight polymer. The high-molecular-weight peak decreased upon decreasing of the Al to V ratio and increased at higher temperatures. The diminished overall polymer productivity observed for the ethylene and 1-octene copolymerization run (Table 1, Entry 5) may be attributed to steric congestion around the vanadium center. It might also result from the formation of dormant sites after the insertion of octene. In situ alkylation of the complex with PMAO and use of $B(C_6F_5)_3$ as a co-activator led to a drop in the overall catalyst productivity as indicated in entry 6. We also observe that this additive suppresses the formation of high-molecular-weight polymer (Figure 5).

The formation of an intense emerald-green color observed upon mixing a solution of the vanadium species **1** with either small or large excess of PMAO cocatalyst clearly indicates the formation of a new species. Reactions carried out in preparative scale by mixing the catalysts and cocatalyst in the ratio 1:2 afforded emerald green crystals of the new trivalent {2,6-bis-[2,6-(i-Pr)$_2$PhN=C(Me)]$_2$(2-MeC$_5$H$_3$N)}VCl$_2$ compound (**2**) (Scheme 1) in reasonable yield (31%). The yield of isolated compound was significantly improved (up to 65%) by concentrating and cooling the reaction mother liquors. The X-ray diffraction pattern of the bulk solid was identical to that of the single crystal, thus confirming the analytical purity of complex **2**. The relatively low yield of isolated crystalline **2** is probably the result of its fairly high solubility. A comparison of the UV−vis spectrum of a freshly prepared solution of analytically pure **2** with that of the mother liquor did not show any significant difference, thus indicating the absence of other vanadium complexes in the reaction mixture. The fact that no other products seem to be present in significant amounts possibly indicates that in contrast to other vanadium-based Ziegler−Natta catalysts,[15] the present system has only little or no possibility of having the ligand abstracted from the vanadium center by the Al cocatalyst. Compound **2** was also conveniently prepared in similar yield upon treatment of **1** with an equimolar amount of MeLi. The magnetic moment calculated for the formulation as determined by the crystal structure was consistent with the high spin d^2 electronic configuration of trivalent vanadium.

(15) (a) Cramail, H.; Dolatkhani, M.; Deffieux, A. *New EPDM's Based on Linear Dienes: Conventional Versus Metallocene Catalysis*; Metallocenes '95 Int. Congr. Metallocene Polym. Scotland Business Research: Skillman, NJ; 1995, pp 227−241. (b) Cann, K. G.; Nicoletti, J. W.; Bai, X.; Hussein, F. D.; Lee, K. H.; Zilker, D. P.; Goeke, G. L. *ACS Polym. Prepr.* **1998**, *39*, 192. (c) Smith, P. D.; Martin, J. L.; Huffman, J. C.; Bansemer, R. L.; Caulton, K. G. *Inorg. Chem.* **1985**, *24*, 2997. (d) Chan, M. C. W.; Cole, J. M.; Gibson, V. C.; Howard, J. A. K. *J. Chem. Soc., Chem. Commun.* **1997**, 2345 and refs therein. (e) Coles, M. P.; Gibson, V. C. *Polym. Bull.* **1994**, *33*, 529. (f) Henrici-Olive, G.; Olive, S. *Angew. Chem., Int. Ed. Engl.* **1971**, *10*, 776. (g) Evens, G. G.; Pijpers, E. M. J.; Seevens, R. H. M. In *Transition Metal Catalyzed Polymerization:* Quirk, R. P., Ed.; Cambridge University Press: Cambridge, 1988; p 782. (h) Doi, Y.; Suzuki, S.; Hizai, G.; Soga, K. In *Transition Metal Catalyzed Polymerization;* Quirk, R. P., Ed.; Cambridge University Press: Cambridge, 1988; p 182. (i) Ver Strate, G. In *Encyclopedia of Polymer Science and Engineering*, 2nd ed.; Wiley: New York, 1985; Vol. 6, p 543.

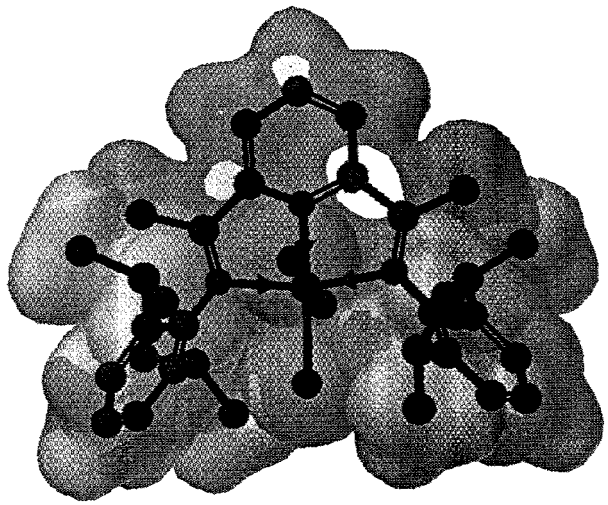

Figure 6. Superimposition of the three-dimensional surface representing the total electronic density distribution over the structure of **1**.

The connectivity of this new vanadium complex, as demonstrated by X-ray crystallography, showed that an important reorganization of the ligand had taken place as a result of the precatalyst/cocatalyst interaction. The formation of **2** is the result of an unusual chloride abstraction reaction by Me-M [M = Li, AlO] where the alkyl group was delivered to one of the two *ortho* carbon atoms of the pyridine ring rather than to the metal center (Scheme 1). As part of the same process, a chlorine atom was removed from vanadium. Thus the reaction resulted in a considerable release of steric hindrance around vanadium which decreased the coordination number by one unit (from 6 to 5) and adopted a trigonal bipyramidal coordination geometry. In the process, the ring acquires a negative charge, and the neutral diimine/pyridine ligand *is transformed into a diimine/anionic amide*. In other words, the interaction of catalyst with cocatalyst results in: (1) the transformation of the ligand in an anionic amide and (2) the creation of an empty coordination site around vanadium. This behavior has two related precedents in the chemistry of zirconium.[16]

There are two possible, different driving forces that combine to push the reaction along this unusual pathway. The total electronic density distribution, as generated by the ZINDO/INDO/1 wave functions calculations (Nucleophilic Susceptibility subroutine of the CaChe software package)[17] was evaluated for a model compound with the atomic coordinates of **1**. Figure 6 shows the superimposition of the three-dimensional surface over one of the two possible resonance structures of **1**. The result of the calculation clearly indicated that the part of the molecule most positively charged and thus more susceptible to nucleophilic attack are indeed the two pyridine *ortho* carbon atoms (Figure 5). In addition, the alkylation of the pyridine ring generated a diene/amido system whose extensive conjugation with the metal center might well provide the stabilization energy necessary to balance the loss of aromaticity of the pyridine ring.[18] In agreement with this proposal, the $V-N_{pyridine}$ distance in complex **2** is significantly shorter than in **1** thus indicating an increase of V−N π-bonding.

As mentioned above, the reaction of **1** with either PMAO, Me_3Al, or MeLi seems to exclusively produce the catalyst precursor **2**. However, only PMAO catalyzes ethylene polymerization since no appreciable olefin polymerization was observed with Me_3Al. The activity of **2** was the same as with complex **1** and produced polymers with the same characteristics and quality.[19] On the basis of these observations, it seems legitimate to conclude that complex **1** is the precursor of **2** which is in turn the precursor of the catalytically active species. The fact that the presence of a cocatalyst is necessary for the catalytic activity of **2** rules out the possibility that the alkylation of the pyridine ring might perhaps be a reversible process with the methyl being transferred to the vanadium atom to start the polymerization reaction.

The possibility that cationic vanadium alkyls or other neutral species with different nuclearity may be the catalytically active species, as well as any other mechanistic possibility is entirely plausible and cannot be ruled out at this stage. Thus, attempts to isolate the catalytically active species were carried out by reacting **2** with excess PMAO. The reactions led only to unreacted **2** with no evidence for the formation of other products. A similar result was obtained at higher temperatures. The solution of mixtures of catalyst/cocatalyst were indefinitely stable in the range 50−100 °C (appreciable decomposition occurred only at 120 °C). In all cases, unreacted **2** was the only detectable compound. Therefore, if the subsequent role of the PMAO cocatalyst, after modifying the di-imino/pyridine ligand, is perhaps that of replacing one or two of the residual chlorine atoms to form the corresponding coordinatively unsaturated vanadium alkyl derivatives, it is well possible that only a small fraction of **2** is actually activated. This observation prompted us to investigate the reaction of **2** with stronger methylating agents. Reaction of either **1** with 4 equiv or of **2** with 3 equiv of MeLi yielded two different compounds which were separated via addition of TMEDA to the reaction mixture (Scheme 2). Workup *in the absence* of TMEDA afforded the unprecedented monovalent and anionic vanadium dialkyl complex {2,6-bis-[2,6-(i-Pr)$_2$PhN=C(Me)]$_2$(C_5H_3N)}V(CH_3)(μ-CH_3)Li(Et_2O)$_3$ (**3**). The most striking feature of this compound is the absence of the methyl group originally present on the pyridine *ortho* carbon atom. The crystallographic features of this compound indicate that the regular geometry of the diimine/pyridine ring was restored during the reaction via elimination of the methyl group, while the vanadium oxidation state was lowered to +1 during the process. The vanadium center bears two methyl groups which, together with the ligand, provide the metal with a strange square pyramidal geometry.[20] The magnetic moment measured for analytically pure samples and calculated according to the formula as provided by the crystal structure indicates that the vanadium atom is in an intermediate-spin d^4 electronic configuration.

The second product that was isolated *upon addition* of TMEDA to the reaction mixture is also an anionic monovalent vanadium dimethyl derivative [{2,6-bis[2,6-(i-Pr)$_2$PhN=C(Me)]$_2$(2,3-$Me_2C_5H_3N$)}V(CH_3)$_2$][Li(THF)$_2$(TMEDA)$_2$] (**4**). One minor difference with respect to **3** is that the lithium countercation is separated and fully solvated by one molecule of TMEDA and two molecules of THF and does not form bonding contacts with the vanadium anionic moiety. The most surprising differ-

(16) (a) Bei, X.; Swenson, D. C.; Jordan, R. F. *Organometallics* **1997**, *16*, 3282. (b) Kobriger, L. M.; McMullen, A. K.; Fanwick, P. E.; Rothwell, I. P. *Polyhedron* **1989**, *8*, 77.

(17) Quantum CAChe 2.0 for Windows software package, Oxford Molecular Group **1997**.

(18) See, for example: Berno, P.; Gambarotta, S. *Organometallics* **1994**, *13*, 2569.

(19) A comparison of the relative activity of **1** and **2** and polymer quality, was obtained by carrying out two simultaneous polymerization experiments by using 5 mM solution of the catalyst, a V/Al = 60 and ethylene P = 1 atm. The two systems produced respectively 6.1 and 6.3 g of polymer in a 20 min run. The polymer quality was also very comparable.

(20) However, the coordination geometry of the vanadium center is very similar to that of the d^6 Fe(II) compound reported by Brookhart.[4]

Scheme 2

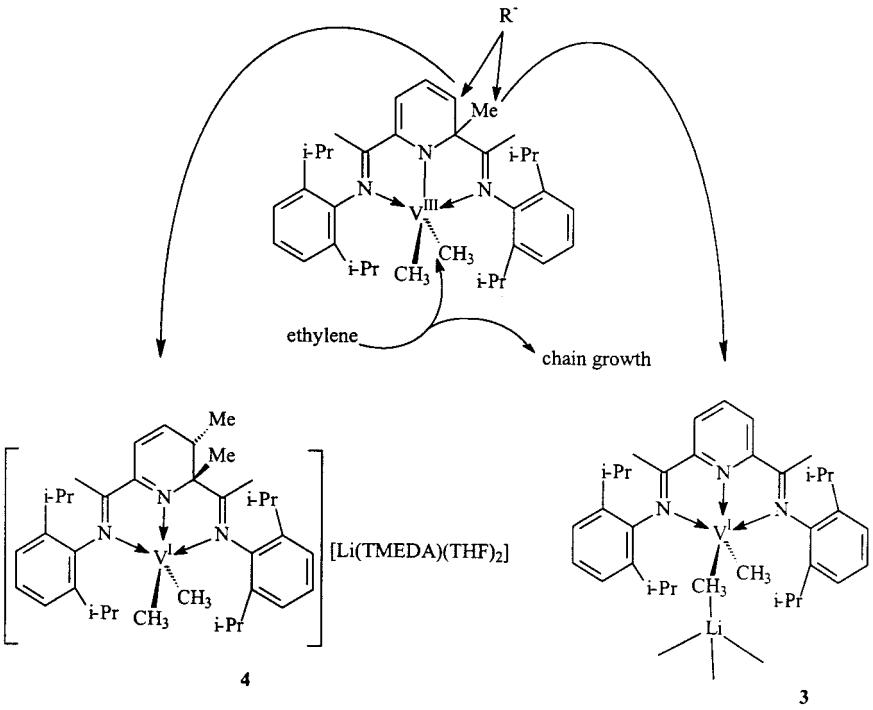

ence, however, is the presence of a *second Me group* on the ring *meta* position adjacent to the already alkylated carbon atoms. The two methyl groups are located on the two opposite sides of the molecular plane (Figure 4). Even in this case, the ligand involvement in the reaction resulted in a two electron reduction of vanadium.

While it is unlikely that simple absence or presence of TMEDA is responsible for driving the reaction toward either the dealkylation or second ring-alkylation pathways, the two compounds **3** and **4** are probably formed by two simultaneous processes. The presence/absence of TMEDA simply afforded crystallization of one species in favor of the other.

In both **3** and **4** the ligand is no longer an anionic organic amide. The ligand was transformed respectively into a neutral diimine/pyridine and a diimine/azadiene ligand. Although these two species are considerably different, both arise from similar two-electron reduction processes of the vanadium atom. The process can be envisioned as the result of a nucleophilic attack on either the methyl group attached to the *ortho* carbon atom, or at the *meta* carbon atom (Scheme 2). In the first case, the attack resulted in methyl abstraction and formation of ethane (identified in the gas chromatogram of the reaction mixture) while the pyridine ring was reformed. Two electrons were transferred in the process from the ring to the vanadium center which consequently reduced its oxidation state from +3 to +1. A similar reduction occurred in the second case during the formation of **4** when a methyl group attacked the ring *meta* position. Even in this case, the reaction implies a two-electron transfer to the vanadium center and consequent reduction to the monovalent state. As expected, the monovalent complexes **3** and **4** either with or without cocatalyst and activators are inert toward ethylene polymerization. Thus, their isolation shows that should a similar process occur (even at minor extent) with milder alkylating agents such as PMAO, this will provide a possible reduction pathway of the metal center with consequent chain termination.

Concluding Remarks

Involvement of the ligand directly in the reactivity of the metal center is the key to understanding the high activity of this catalytic system. First of all, the alkylation of the pyridine ring transforms the initial coordination complex **1** into a covalent transition metal amide **2,** the process being accompanied by a decrease in the coordination number of the metal center. Steric hindrance is probably the factor responsible for the very poor comonomer incorporation observed with this system. Further attack on the ligand, which reduces the metal toward an inactive V(I) species, is very fast with MeLi and might also occur at smaller extent with PMAO. Finally, despite its involvement in the reactivity of the metal center, the ligand is strongly bound to the transition metal with no evidence that it could be abstracted by the Al cocatalyst. This is certainly an important factor which, in combination with the unique ability of this ligand to stabilize vanadium alkyls, is probably responsible for the high activity observed in this system.

Acknowledgment. This work was supported by the Natural Science and Engineering Council of Canada (NSERC) and NATO. Drs. John McMeeking and Daryll Harrison (NOVA Chemicals Corporation) are gratefully acknowledged for useful discussions.

Supporting Information Available: Listing of atomic coordinates, thermal parameters, bond distances and angles for **1**, **2, 3** and **4** (PDF). This material is available free of charge via the Web at http://pubs.acs.org.

JA990263X